SRC TR 88-50

On The Conceptual Design Of A Novel Class Of Robot Configurations

by

L.-W. Tsai and F. Freudenstein

ON THE CONCEPTUAL DESIGN OF A NOVEL CLASS OF ROBOT CONFIGURATIONS

by

Lung-Wen Tsai*

and

Ferdinand Freudenstein**

* Associate Professor of Mechanical Engineering and Systems Research Center, University of Maryland, College Park, MD, 20742; Mem. ASME

** Higgins Professor of Mechanical Engineering, Columbia University, New York, NY 10027; Fellow, ASME

ABSTRACT

The conceptual design has been investigated of the kinematic structure of relatively small robots with positive, rigid-body drive elements of minimum complexity in order to maximize rigidity, minimize vibrations and response time and optimize payload. Several novel robot configurations have been conceived and their displacement analysis and static torque analysis derived directly from their kinematic structure. It is believed that these configurations can be advantageous in the design of high-performance robots relative to current designs involving cables and push/pull elements.

INTRODUCTION

The design of relatively small robots is generally governed by the need for simplicity, minimization of the number of moving elements and cost-effectiveness. For this reason cable and push/pull elements are commonly used. As a result, however, vibrations and backlash are relatively large, while the payload is quite limited. While such designs are acceptable in some applications, such as classroom instruction, it would seem that for many industrial applications a more positive and rigid construction is desirable. In the light of these considerations we have conceived several novel robot configurations with single-loop, rigid drive elements and investigated their structural characteristics, displacement equations and static torque analysis. This has involved both the creative design methodology and the design analysis based on kinematic structure, as well as considerations involving mechanical construction. It is believed that the configurations which will be described have the potential for improved robot performance.

The design of the end effector has not been included. If a cable drive for the end effector is acceptable, current designs can be used. If not, various possibilities exist ranging from separate non-coaxial motors for each degree of freedom of the end effector to a robot concept such as the Bendix [1] or Cincinnati-Milacron [4] three-degree-of-freedom wrist.

THE KINEMATIC STRUCTURE OF RELATIVELY SMALL ROBOTS WITH RIGID-BODY ACTUATORS-GENERAL

We consider only the simplest rotary drive elements i.e.: those based on the simplest single-degree-of-freedom linkages with turning pairs and prismatic pairs and/or spur and bevel-gearing. As is well known there are seven basic linkage mechanisms in the first category: Cardanic motion and its inverse, the Scotch yoke, the swinging and turning blocks, the slider-crank, the four-bar linkage and the Rapson slide. Of these practical designs (other than those involving gearing) are limited to the parallel equal-crank linkage (the tie-rod drive). The antiparallel equal-crank linkage is not practical because of the dead center positions.

An ingenious modification of this linkage (Figs. 1a,b,c), however, has been described by S. Sh. Blokh [3]. This results in a compact positive drive, as shown in Fig. 1d, which will be described in greater detail subsequently, and which can be adapted to robot configurations as well.

The quality of any particular mechanism, however, is a function not only of its kinematic structure, but also of the ability to proportion the mechanism for the given applied loads within the available space. The displacement, torque and force analyses required for this task are often far from elementary. In the development which follows, therefore, we have also applied recent developments in the displacement and torque analysis directly derived from kinematic structure [5]. This in turn should facilitate the evaluation of the configurations which will be described.

(i) <u>3R robot with positive (-1:1) drive</u>

Figure 1c shows a swinging-block linkage, ABCD, with crank r=OA, coupler ABC=b and swinging-block pivoted at B (OB=a).

The trajectory of point C of coupler AC has been optimized by Blokh [3] according to the theory of structural-error optimization, so that the trajectory of point C deviates as little as possible from a circle.

The optimum proportions derived by Blokh are as follows:

$$b = \frac{1}{4}[5a + 3\sqrt{a^2-r^2}]$$

$$c = \frac{a[5a + 3\sqrt{a^2-r^2}]}{3a + \sqrt{a^2-r^2}} \qquad (1)$$

$$R^2 = r^2 + \frac{L_1^{\,2}}{4r^2}$$

$$\text{where } L_1 = \frac{r[5a + 3\sqrt{a^2-r^2}][\sqrt{a^2-r^2} - a]}{2[3a + \sqrt{a^2-r^2}]}$$

If $\lambda = r/a$, it can be shown that the maximum difference (dr) between the trajectory of point C and the circle center D and radius r is given very nearly by the expression;

$$\frac{dr}{r} = \frac{[5 + 3\sqrt{1-\lambda^2}]^2[\sqrt{1-\lambda^2}-1]^2}{32\lambda^2[3 + \sqrt{1-\lambda^2}]^2} \qquad (2)$$

Hence, if r = 20 mm and a = 200 mm - a representative case in robot applications - this gives dr ≈ 0.005 mm - a negligible quantity.

The corresponding schematic robot arm design is shown in Fig. 1d. The linkage functions as an antiparallel equal-crank linkage, but the proportions are in effect optimized so that the swinging block, B, (which ensures positive

guidance at all times) will not interfere with the motion of the linkage. Figure 1e illustrates the construction of a robot arm of the above type.

Any robot with tie-rods (i.e.: with the parallel equal-crank linkage) can also be configured with the above-mentioned counter-rotating drive (-1:1) for all or some of the arms. The -1:1 drive is sturdy (as enhanced by the swinging block) and there is no need for a dual drive (as in the tie-rod construction) in order to maintain positive guidance.

(ii) 3R robot with a spur-gear drive and tie rods

Figure 2 shows a schematic of a three-degree-of-freedom robot with a rotating base, an input disc, S, and two tie-rods providing the parallel drive to the intermediate gear, which connects with the planet or end effector, which is also guided by arm ABC. Input motors (not shown) rotate the base about a vertical axis, and arm ABC and input disk S about the horizontal axis through A.

If the base is stationary the drive reduces to a two-degree-of-freedom gear train, the inputs being the rotation (θ_A) of the arm and the rotation (θ_S) of the input disk.

A kinematic analysis of the planetary drive yields the following displacement equation: if θ_P, θ_A, θ_S denote the rotations of end effector, arm and input disk, respectively,

$$\theta_P = \theta_A \left(\frac{R_S}{R_P} + 1\right) - \frac{\theta_S R_S}{R_P} \tag{3}$$

where R_S, R_P denote the pitch radii of input disk and planet gear, respectively. The first term of eq. (3) corresponds to the classical case in which the input disk is stationary, while the second term (which is new) accounts

for the rotation of the disk. If the rotations of the arm and end effector occur at constant angular velocities, we obtain trochoidal trajectories of point P of the end effector. In the general case, however, in which the gear ratio is not constant, the trajectory is arbitrary within the reach of the robot. The drive motor for the rotating base would be grounded while the other two motors could be mounted horizontally and coaxially on the base plate. The robot comprises 8 links and 10 joints. Note that the tie-rods have replaced the cables and that robot operation is positive at all times.

(iii) 3R and 4R robot configurations with crankshaft and without gears

A seven-link robot with different construction (while retaining the tie-rod drive) is shown in Fig. 3. Tie-rods 5 and 6 are actuated by crankshaft 3, two of the drive motors being coaxial with it. The end effector is integral with the second crankshaft. This construction avoids the use of gears, while retaining the tie-rod guidance. The principle can be extended to the design of an 11-link 4R robot, as shown in Fig. 4. In this design the fourth motor is mounted on a floating link.

(iv) 3R robot with bevel-gear actuation of tie rods

Figure 5a shows a 3R robot with tie-rod construction, utilizing a bevel-gear drive with all motors ground connected (the motors are not shown). In order to facilitate the evaluation and optimization of this drive we consider the displacement and static torque analysis as follows.

(a) Displacement analysis

The drive has 12 links, 13 turning pairs and 5 gear pairs. It has two four-bar loops phased 90° apart (one of which is redundant). For purposes of

kinematic analysis we may, therefore, neglect one of the tie-rods and the associated joints. Hence, we effectively have 11 links, 11 turning pairs and 5 gear pairs. The degree of freedom of the mechanism, F, can be determined as follows:

$$F = \lambda(\ell - j - 1) + \sum f_i \tag{4}$$

where ℓ = number of links,

j = number of joints

$\sum f_i$ = summation of joint freedoms

λ = mobility number = 3.

Note that although this drive (and the one which follows) has mixed plane/spherical motions, λ=3 in both cases and the general degree-of-freedom equation remains applicable with λ=3. Hence F = 3(11-16-1) + 11 + (2)(5) = 3. All motors are ground connected. For displacement-analysis purposes we note that the relative rotation of crankshaft 8 with respect to arm 7 is identical to that of crankshaft 10 with respect to arm 7. Furthermore, the "equivalent open-loop chain" [5] of this mechanism is the chain 0-4-7-10. If $\theta_{i,j}$ denotes the rotation of link i relative to link j, we need to determine $\theta_{10,7}$, $\theta_{7,4}$ and $\theta_{4,0}$. These can be obtained from the following fundamental-circuit equations for bevel-gear trains [5] and the graph of Fig. 5b:

Circuit (8,6) (4): $$\theta_{8,4} = N_{68}\theta_{6,4} \tag{5}$$

" (7,5) (4): $$\theta_{7,4} = -N_{57}\theta_{5,4} \tag{6}$$

" (3,6) (0): $$\theta_{6,0} = -N_{36}\theta_{3,0} \tag{7}$$

" (2,5) (0): $$\theta_{5,0} = -N_{25}\theta_{2,0} \tag{8}$$

" (1,4) (0): $$\theta_{4,0} = -N_{14}\theta_{1,0} \tag{9}$$

where $N_{ij} = N_i/N_j$ denotes the gear ratio of gears i and j with N_i and N_j teeth, respectively, and $\theta_{i,j}$ denotes the rotation of link i relative to link j.

From the four-bar loop, we have

$$\theta_{10,7} = \theta_{8,7} \tag{10}$$

The coaxiality conditions are:

$$\theta_{5,4} = \theta_{5,0} - \theta_{4,0} \tag{11}$$

$$\theta_{6,4} = \theta_{6,0} - \theta_{4,0} \tag{12}$$

and

$$\theta_{8,4} = \theta_{8,7} - \theta_{4,7} \tag{13}$$

Substituting (7) and (9) into (12) and substituting the resulting equation into (5), we have

$$\theta_{8,4} = N_{68}(-N_{36}\theta_{3,0} + N_{14}\theta_{1,0}) \tag{14}$$

Substituting (13) into (14) and solving for $\theta_{8,7}$, we obtain:

$$\theta_{8,7} = \theta_{4,7} + N_{68}(-N_{36}\theta_{3,0} + N_{14}\theta_{1,0}) \tag{15}$$

Substituting (8) and (9) into (11), and the resulting equation into (6), we have:

$$\theta_{7,4} = N_{57}(N_{25}\theta_{2,0} - N_{14}\theta_{1,0}) \tag{16}$$

since $\theta_{4,7} = -\theta_{7,4}$, we can eliminate $\theta_{4,7}$ from (15) and (16):

$$\theta_{8,7} = -N_{57}(N_{25}\theta_{2,0} - N_{14}\theta_{1,0}) - N_{68}(N_{36}\theta_{3,0} - N_{14}\theta_{1,0}) \tag{17}$$

or

$$\theta_{10,7} = (N_{57} + N_{68})N_{14}\theta_{1,0} - N_{57}N_{25}\theta_{2,0} - N_{68}N_{36}\theta_{3,0} \tag{18}$$

Expressing eqs. (9), (16) and (18) in matrix form we have:

$$\begin{bmatrix} \theta_{4,0} \\ \theta_{7,4} \\ \theta_{10,7} \end{bmatrix} = \begin{bmatrix} -N_{14} & 0 & 0 \\ -N_{14}N_{57} & N_{25}N_{57} & 0 \\ (N_{57}+N_{68})N_{14} & -N_{25}N_{57} & -N_{36}N_{68} \end{bmatrix} \begin{bmatrix} \theta_{1,0} \\ \theta_{2,0} \\ \theta_{3,0} \end{bmatrix} \tag{19}$$

Equation (19) relates the joint angles to the input angles.

If $N_{57} = N_{68}$ and $N_{14} = N_{25} = N_{36}$, then eq. (19) reduces to:

$$\begin{bmatrix} \theta_{4,0} \\ \theta_{7,4} \\ \theta_{10,7} \end{bmatrix} = N_{14} \begin{bmatrix} -1 & 0 & 0 \\ -N_{57} & N_{57} & 0 \\ 2N_{57} & -N_{57} & -N_{57} \end{bmatrix} \begin{bmatrix} \theta_{1,0} \\ \theta_{2,0} \\ \theta_{3,0} \end{bmatrix} \tag{20}$$

Hence we conclude the following:

* $\theta_{4,0}$ is locked when $\theta_{1,0}$ is constant (motor 1 is held stationary);
* The second joint is locked ($\dot{\theta}_{7,4}=0$) when $\dot{\theta}_{1,0}=\dot{\theta}_{2,0}$, or when motors 1 and 2 are driven at the same rate;
* The second and third joints are locked when motors 1,2,3 are driven at the same rate.

Once the joint angles ($\theta_{4,0}$, $\theta_{7,4}$ and $\theta_{10,7}$) are determined, the position of the end-effector can be obtained from the forward kinematics of the equivalent open-loop manipulator.

If, on the other hand, the position of the end-effector is given, we can determine the joint angles from the inverse kinematics of the equivalent open-loop manipulator, and the input angles $\theta_{1,0}$, $\theta_{2,0}$ and $\theta_{3,0}$ from the inverse transformation of eq. (20).

(b) Static torque analysis

Taking the time derivatives of eq. (20) yields:

$$\begin{bmatrix} \dot{\theta}_{4,0} \\ \dot{\theta}_{7,4} \\ \dot{\theta}_{10,7} \end{bmatrix} = N_{14} \begin{bmatrix} -1 & 0 & 0 \\ -N_{57} & N_{57} & 0 \\ 2N_{57} & -N_{57} & -N_{57} \end{bmatrix} \begin{bmatrix} \dot{\theta}_{1,0} \\ \dot{\theta}_{2,0} \\ \dot{\theta}_{3,0} \end{bmatrix} \tag{21}$$

Let $T_{4,0}$, $T_{7,4}$ and $T_{10,7}$ denote the joint torques of the equivalent open-loop chain 0-4-7-10, and let T_1, T_2 and T_3 represent the torques required at drives 1, 2 and 3 respectively. Then from the principle of conservation of energy, we have:

$$[T_{4,0}\ T_{7,4}\ T_{10,7}] \begin{bmatrix} \dot{\theta}_{4,0} \\ \dot{\theta}_{7,4} \\ \dot{\theta}_{10,7} \end{bmatrix} = [T_1\ T_2\ T_3] \begin{bmatrix} \dot{\theta}_{1,0} \\ \dot{\theta}_{2,0} \\ \dot{\theta}_{3,0} \end{bmatrix} \tag{22}$$

Substituting (21) into (22), yields;

$$\{N_{14}[T_{4,0}\ T_{7,4}\ T_{10,7}] \begin{bmatrix} -1 & 0 & 0 \\ -N_{57} & N_{57} & 0 \\ 2N_{57} & -N_{57} & -N_{57} \end{bmatrix} -[T_1\ T_2\ T_3]\} \begin{bmatrix} \dot{\theta}_{1,0} \\ \dot{\theta}_{2,0} \\ \dot{\theta}_{3,0} \end{bmatrix} = [0] \tag{23}$$

Hence,

$$N_{14}[T_{4,0}\ T_{7,4}\ T_{10,7}] \begin{bmatrix} -1 & 0 & 0 \\ -N_{57} & N_{57} & 0 \\ 2N_{57} & -N_{57} & -N_{57} \end{bmatrix} -[T_1\ T_2\ T_3] = [0] \tag{24}$$

Taking the transpose of (24) yields:

$$\begin{bmatrix} T_1 \\ T_2 \\ T_3 \end{bmatrix} = N_{14} \begin{bmatrix} -1 & -N_{57} & 2N_{57} \\ 0 & N_{57} & -N_{57} \\ 0 & 0 & -N_{57} \end{bmatrix} \begin{bmatrix} T_{4,0} \\ T_{7,4} \\ T_{10,7} \end{bmatrix} \tag{25}$$

Equation (25) relates the joint torques to the input torques. Note that the torque exerted on link 8 is the same as that exerted on link 10. The joint torques $T_{4,0}$, $T_{7,4}$ and $T_{10,7}$ in the equivalent open-loop chain, however, do not represent the torques exerted on links 4, 7 and 10.

Taking the inverse of eq. (25), we obtain

$$\begin{bmatrix} T_{4,0} \\ T_{7,4} \\ T_{10,7} \end{bmatrix} = N_{41} \begin{bmatrix} -1 & -1 & -1 \\ 0 & N_{75} & -N_{75} \\ 0 & 0 & -N_{75} \end{bmatrix} \begin{bmatrix} T_1 \\ T_2 \\ T_3 \end{bmatrix} \tag{26}$$

where $N_{41} = 1/N_{14}$ and $N_{75} = 1/N_{57}$. The torques exerted in links 4, 5, and 6 are given by

$$T_4 = - N_{41}T_1 \tag{27}$$

$$T_5 = - N_{52}T_2 = - N_{41}T_2 \tag{28}$$

$$T_6 = - N_{63}T_3 = - N_{41}T_3 \tag{29}$$

Substituting (27)-(29) into the first row of (26) yields,

$$T_{4,0} = T_4 + T_5 + T_6 \tag{30}$$

Hence, we conclude that the torque, $T_{4,0}$, is equal to the sum of the torques T_4, T_5 and T_6 exerted on links 4, 5, and 6. Similarly, the torques T_7 and T_8 exerted on links 7 and 8, respectively, are given by

$$T_7 = -N_{75}T_5 = N_{41}N_{75}T_2 \tag{31}$$

$$T_8 = N_{86}T_6 = -N_{41}N_{86}T_3 \tag{32}$$

Substituting (31) and (32) into the second row of (26) yields

$$T_{7,4} = T_7 + T_8 \tag{33}$$

Hence, the joint torque, $T_{7,4}$, is equal to the sum of the torques exerted by links 7 and 8. The forces on the tie-rods are indeterminate. The sizing of the links of the drive can now be completed.

(v) <u>3R robot with bevel-gear drive</u>

An alternative 3R design, in which the tie-rods and crankshaft are replaced by a bevel-gear drive, is shown in Fig. 6a, the graph of which is shown in Fig. 6b. This is a six-link mechanism with three inputs ($\theta_{1,0}$, $\theta_{2,1}$ and $\theta_{4,2}$) and link 3 is the end effector. The displacement analysis follows.

The mechanism has 6 links, 5 turning pairs and 2 gear pairs corresponding to a degree of freedom, F, given by F = 3(6-7-1)+ 5 +(2)(2) = 3.

(a) <u>Displacement analysis</u>

The equivalent open-loop chain of the drive consists of links 0-1-2-3. We proceed as previously in terms of the fundamental circuits of the system.

Fundamental circuits	Displacement equations	
(4,5) (2)	$\theta_{4,2} = -N_{54}\theta_{5,2}$	(34)
(5,3) (2)	$\theta_{5,2} = N_{35}\theta_{3,2}$	(35)
Substituting (34) into (35), we have:	$\theta_{4,2} = -N_{54}N_{35}\theta_{3,2}$	(36)

Hence the joint angles are related to the inputs as follows:

$$\begin{bmatrix} \theta_{1,0} \\ \theta_{2,1} \\ \theta_{4,2} \end{bmatrix} = \begin{bmatrix} 1 & 0 & 0 \\ 0 & 1 & 0 \\ 0 & 0 & -N_{54}N_{35} \end{bmatrix} \begin{bmatrix} \theta_{1,0} \\ \theta_{2,1} \\ \theta_{3,2} \end{bmatrix} \tag{37}$$

where $N_{ij} = N_i/N_j$ denotes the gear ratio of gears i and j with N_i and N_j teeth, respectively.

(vi) <u>3R robot with bevel-gear drive - version 2</u>

And finally we consider a further refinement (shown in Fig. 7) of the bevel-gear actuated 3R robot in which all motors are connected to ground. This is a 10-link robot (excluding ground). It will suffice here to summarize the displacement and static torque analysis.

(a) <u>Displacement analysis</u>

The fundamental-circuit equations are, in addition to eqs. (34) and (35), as follows:

Fundamental circuits	Displacement equations	
(4,7) (1)	$\theta_{4,1} = N_{74}\theta_{7,1}$	(38)
(2,6) (1)	$\theta_{2,1} = -N_{62}\theta_{6,1}$	(39)

The coaxiality conditions are given by

$$\theta_{7,1} = \theta_{7,0}-\theta_{1,0} \tag{40}$$

and

$$\theta_{6,1} = \theta_{6,0}-\theta_{1,0} \tag{41}$$

Substituting (40) into (38), we have

$$\theta_{4,1} = N_{74}(\theta_{7,0}-\theta_{1,0}) \tag{42}$$

Substituting (41) into (39), we have

$$\theta_{2,1} = -N_{62}(\theta_{6,0}-\theta_{1,0}) \tag{43}$$

But $\theta_{4,2} = -N_{54}N_{35}\theta_{3,2}$(eq.36) (44)

and $\theta_{4,2} = \theta_{4,1}-\theta_{2,1}$ (45)

Solving (42), (44) and (45) for $\theta_{7,0}$, we have

$$\theta_{7,0} = \theta_{1,0}+N_{47}\theta_{2,1}-N_{47}N_{54}N_{35}\theta_{3,2} \tag{46}$$

Solving (43) for $\theta_{6,0}$ we find

$$\theta_{6,0} = \theta_{1,0}-N_{26}\theta_{2,1} \tag{47}$$

Hence the joint angles are related to angles $\theta_{1,0}$, $\theta_{6,0}$ and $\theta_{7,0}$ as follows:

$$\begin{bmatrix}\theta_{1,0}\\ \theta_{6,0}\\ \theta_{7,0}\end{bmatrix} = \begin{bmatrix}1 & 0 & 0\\ 1 & -N_{26} & 0\\ 1 & N_{47} & -N_{47}N_{54}N_{35}\end{bmatrix}\begin{bmatrix}\theta_{1,0}\\ \theta_{2,1}\\ \theta_{3,2}\end{bmatrix} = [A]\begin{bmatrix}\theta_{1,0}\\ \theta_{2,1}\\ \theta_{3,2}\end{bmatrix} \tag{48}$$

We can relate $\theta_{1,0}$, $\theta_{6,0}$ and $\theta_{7,0}$ to the inputs as follows:

$$\theta_{1,0} = -N_{81}\theta_{8,0} \tag{49}$$

$$\theta_{6,0} = -N_{96}\theta_{9,0} \tag{50}$$

$$\theta_{7,0} = -N_{10,7}\theta_{10,0} \tag{51}$$

Hence the overall transformation yielding the angular displacements of the system is as follows:

$$\begin{bmatrix} \theta_{8,0} \\ \theta_{9,0} \\ \theta_{10,0} \end{bmatrix} = \begin{bmatrix} -N_{18} & 0 & 0 \\ -N_{69} & N_{69}N_{26} & 0 \\ -N_{7,10} & -N_{7,10}N_{47} & N_{7,10}N_{47}N_{54}N_{35} \end{bmatrix} \begin{bmatrix} \theta_{1,0} \\ \theta_{2,1} \\ \theta_{3,2} \end{bmatrix} = [B] \begin{bmatrix} \theta_{1,0} \\ \theta_{2,1} \\ \theta_{3,2} \end{bmatrix} \tag{52}$$

(b) <u>Static torque analysis: torque at motor pinion</u>

Let $T_{1,0}$, $T_{2,1}$ and $T_{3,2}$ denote the joint torques in the equivalent open-loop chain; let T_1, T_6 and T_7 denote the torques exerted on links 1, 6 and 7; and let T_8, T_9 and T_{10} denote the torques required at motors 8, 9 and 10, respectively. Then, following the same procedure described in the previous section, we obtain:

$$\begin{bmatrix} T_{1,0} \\ T_{2,1} \\ T_{3,2} \end{bmatrix} = A^T \begin{bmatrix} T_1 \\ T_6 \\ T_7 \end{bmatrix} = \begin{bmatrix} 1 & 1 & 1 \\ 0 & -N_{26} & N_{47} \\ 0 & 0 & -N_{47}N_{54}N_{35} \end{bmatrix} \begin{bmatrix} T_1 \\ T_6 \\ T_7 \end{bmatrix} \tag{53}$$

or

$$\begin{bmatrix} T_{1,0} \\ T_{2,1} \\ T_{3,2} \end{bmatrix} = B^T \begin{bmatrix} T_8 \\ T_9 \\ T_{10} \end{bmatrix} \tag{54}$$

From the first row of eq. (53) we observe that the first-joint torque, $T_{1,0}$, is equal to the sum of torques exerted by links 1, 6 and 7. The torques exerted by links 2 and 4 are given by

$$T_2 = -N_{26}T_6 \tag{55}$$

and $$T_4 = N_{47}T_7 \tag{56}$$

Substituting eqs. (55) and (56) into the second row of eq. (53), yields

$$T_{2,1} = T_2 + T_4 \tag{57}$$

Hence, the second-joint torque is equal to the sum of torques exerted on links 2 and 4.

DISCUSSION

The design concepts which have been described, demonstrate the feasibility of designing drives for relatively small robots with positive link guidance (i.e. guidance without cables or push/pull arrangements). All joints have surface or line contact and the links are rigid. Tie-rod guidance seems well suited for controlling rotations, as do bevel-gear arrangements. And the designs can be optimized for maximizing the number of grounded (motor) inputs. The range of motion can be substantial and the designs can be compact.

It is realized that the weight, number of parts and cost may be greater than for cable-driven robots. However, with the increased performance requirements in terms of rigidity and accuracy - as well as payload - more sophisticated robot designs would seem inevitable.

As far as the end-effector design is concerned, it has been pointed out previously that rigid wrists have been developed and these can be used if the application so indicates. The tie-rod-drive robot configuration shown in Fig. 3 is functionally similar to the "Five-bar parallel-drive arm" of Asada and Youcef - Toumi [2]. In order to maintain reasonably good force transmission however, the range of rotation in the third joint of this arm needs to be

limited to approximately 90°. Another example involves the GMF Robotics Series S-380R "parallel-mechanism" robot. The double tie-rods, crankshafts and arm in Fig. 3 form two parallelograms with one redundant drive. Torque can be transmitted through either tie-rod, which permits the crankshafts to rotate 360° (if desired) without impairing force transmission.

The kinematic and static analysis of rather complicated mechanical systems, consisting of both spatial bevel-gear trains and bar-linkages, can readily be accomplished with the aid of the fundamental-circuit equations obtained directly from their kinematic structure, as introduced by Tsai [5]. We believe that this method of kinematic analysis is not yet generally known by the design profession. In this investigation it is particular helpful in assessing feasibility and size.

The 3R robot configuration shown in Fig. 6a is simple and can be used to replace the parallel mechanism suggested by Asada and Youcef-Toumi [2]. The configuration shown in Fig. 7 is more complicated, but it does permit all motors to be ground connected. Of course it is also possible to consider a design in which only two motors are ground connected while the third motor is mounted on the first moving link (link 1).

CONCLUSION

In the spirit of increased emphasis on the quality of robot performance, several novel robot configurations have been conceived with positive drives to the end effector, so as to maximize rigidity, payload and minimize vibrations. The displacement and torque analyses have been derived as well. The designs are conceived as representative rather than exhaustive and as intermediate between the cable-driven minirobots and large industrial robots with individual

motors at each joint. It is hoped that the concepts which have been described will facilitate such design efforts.

ACKNOWLEDGMENT

This research was supported in part by the Systems Research Center of the University of Maryland via NSF grant No. NSF-8500108.

FIGURES

Fig. 1a,b,c,d,e. Development of robot arm actuator based on modification of antiparallel equal-crank-linkage.

Fig. 2. Geared 3R robot drive with tie-rods.

Fig. 3. 3R robot with crankshaft and tie-rod elements.

Fig. 4. 4R robot with crankshafts and tie-rod elements.

Fig. 5a. Bevel-gear actuated 3R robot with crankshaft and tie-rod elements.

Fig. 5b. Graph of robot drive of Fig. 5a.

Fig. 6a. Bevel-ger actuated 3R robot.

Fig. 6b. Graph of robot drive of Fig. 6a.

Fig. 7. Bevel-gear actuated 3R robot with grounded motors (Version 2).

REFERENCES

1. Anonymous, "Bevel-Gears Make Robot's Wrist More Flexible", Machine Design, Vol. 54, No. 18, Aug. 1982, p. 55.

2. Asada, H. and Youcef-Toumi, K., "Analysis and Design of a Direct-Drive Arm with a Five-Bar-Link Parallel Drive Mechanism", ASME J. of Dynamic Systems, Measurement and Control, Vol. 106, No. 3, Sept. 1984, pp. 225-230.

3. Blokh, S. Sh., "Angenäherte Synthese von Mechanismen", Verlag Technik, Berlin, 1951; translated from Russian by G. Panschin.

4. Stackhouse, T., "A New Concept in Wrist Flexibility", Proceedings of the 9th Int. Symposium on Industrial Robots, Washington, D.C., pp. 589-599, 1979.

5. Tsai, L.W., "The Kinematics of Spatial Robotic Bevel-Gear Trains", Proceedings of the 1987 IEEE Int. Conference on Robotics and Automation, Raleigh, N. Carolina; IEEE Journal of Robotics and Automation, Vol. 4, No. 2, April 1988.

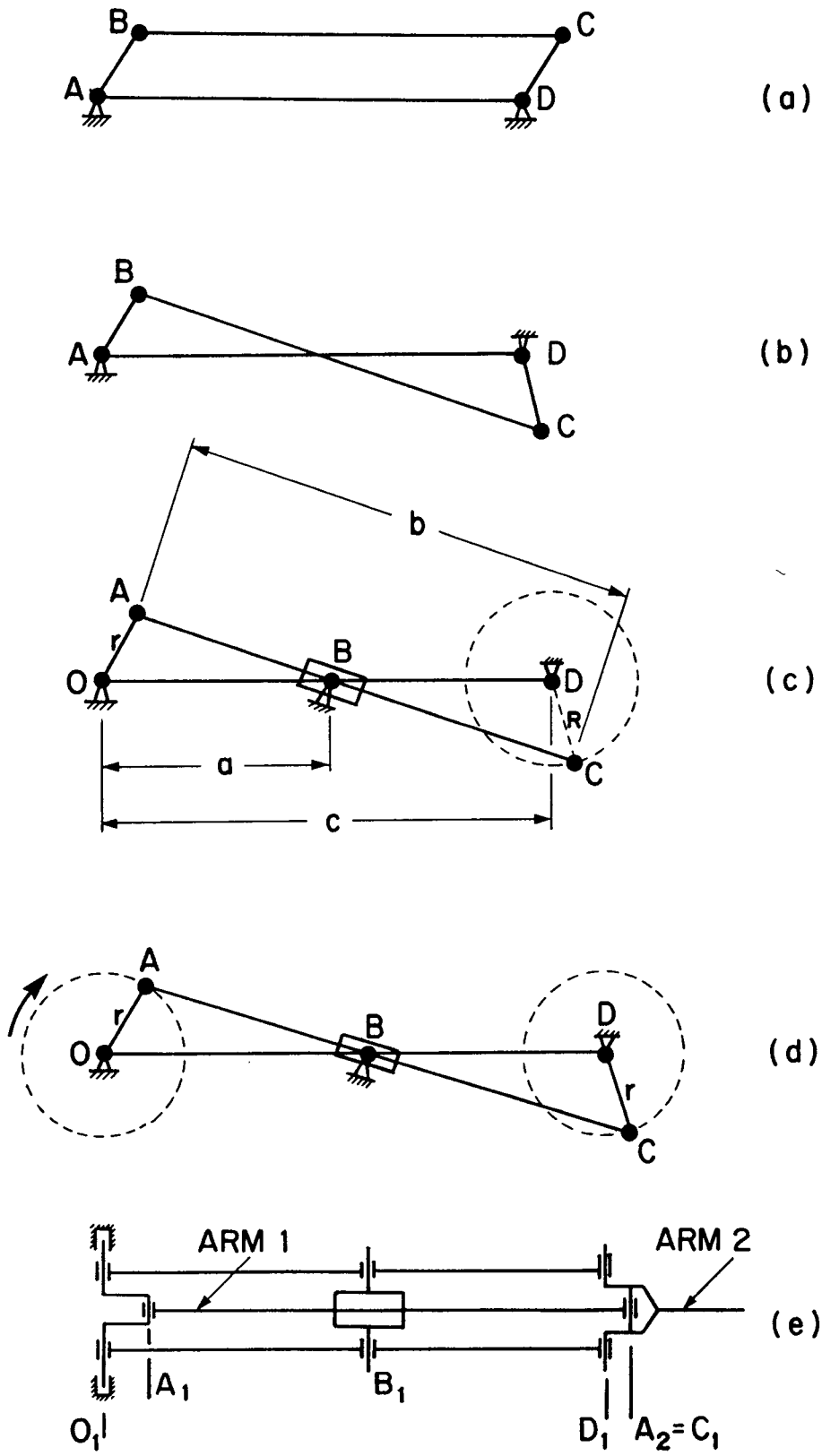
B
C
A
D
(a)
B
A
D
C
(b)
b
A
r
B
O
D
R
C
a
c
(c)
A
r
B
D
O
r
C
(d)
ARM 1
ARM 2
(e)
A1
B1
O1
D1
A2=C1

Fig. 1

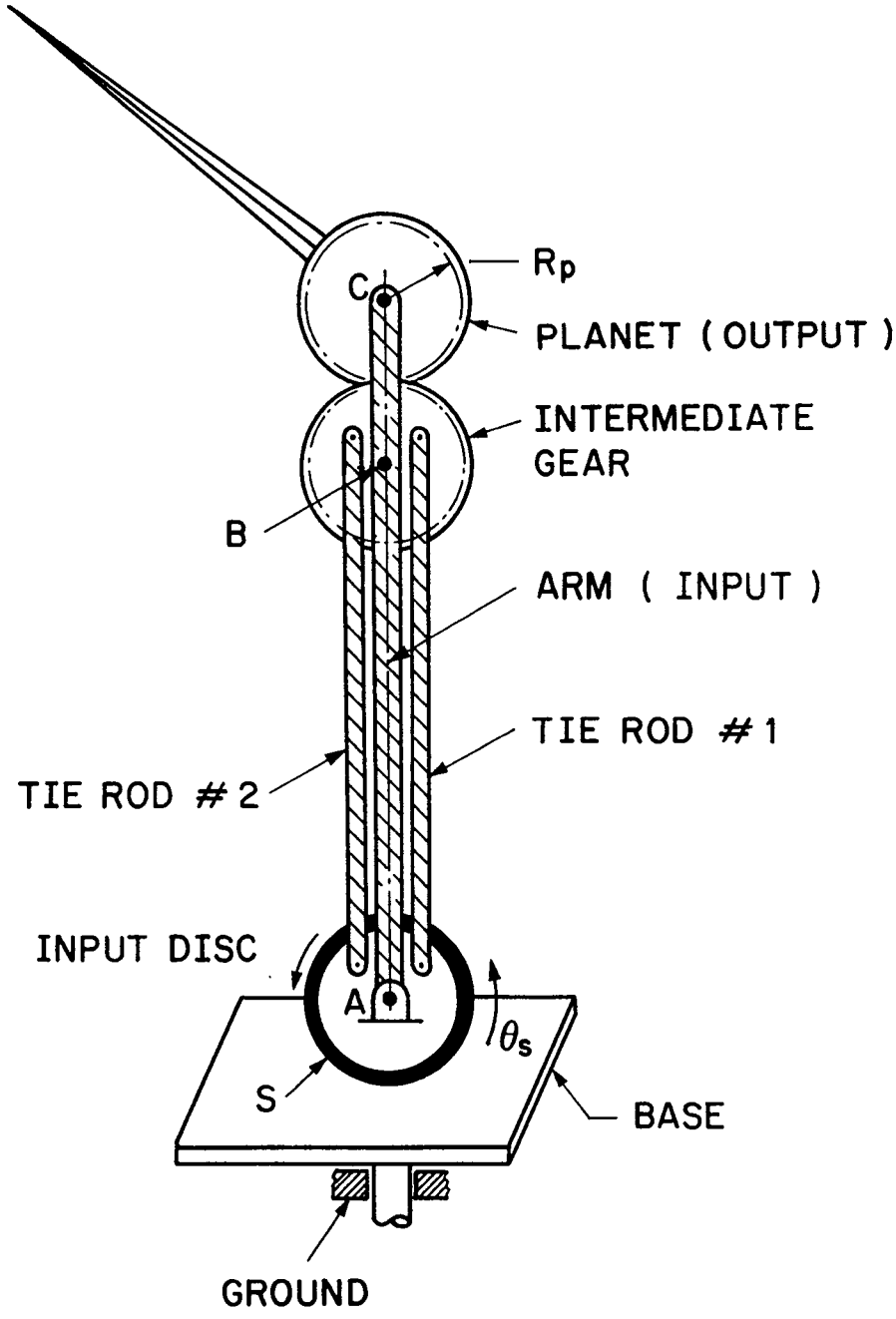
Rp
C
PLANET (OUTPUT)
INTERMEDIATE
GEAR
B
ARM (INPUT)
TIE ROD # 1
TIE ROD # 2
INPUT DISC
A
θs
S
BASE
GROUND

Fig. 2

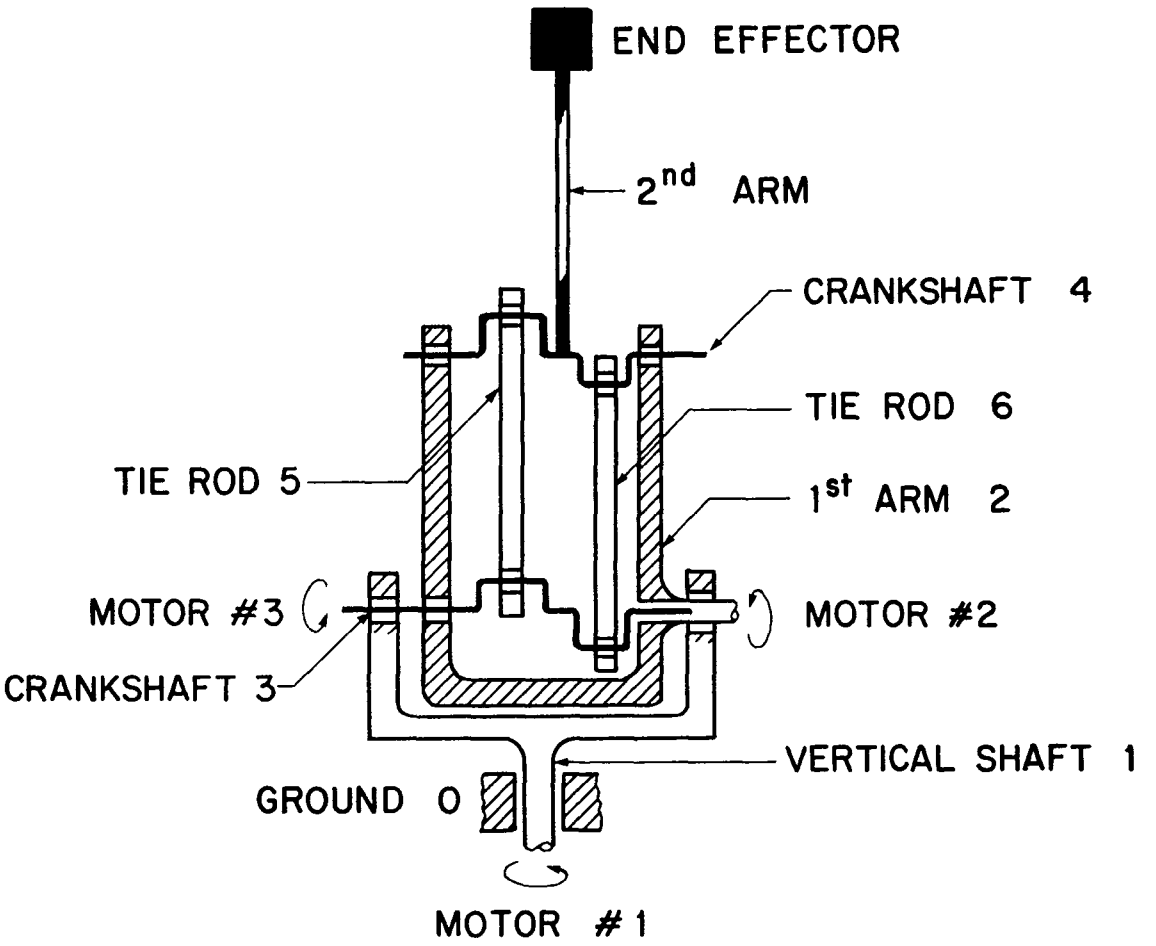
END EFFECTOR
2nd ARM
CRANKSHAFT 4
TIE ROD 6
TIE ROD 5
1st ARM 2
MOTOR #3
MOTOR #2
CRANKSHAFT 3
VERTICAL SHAFT 1
GROUND 0
MOTOR #1

Fig. 3

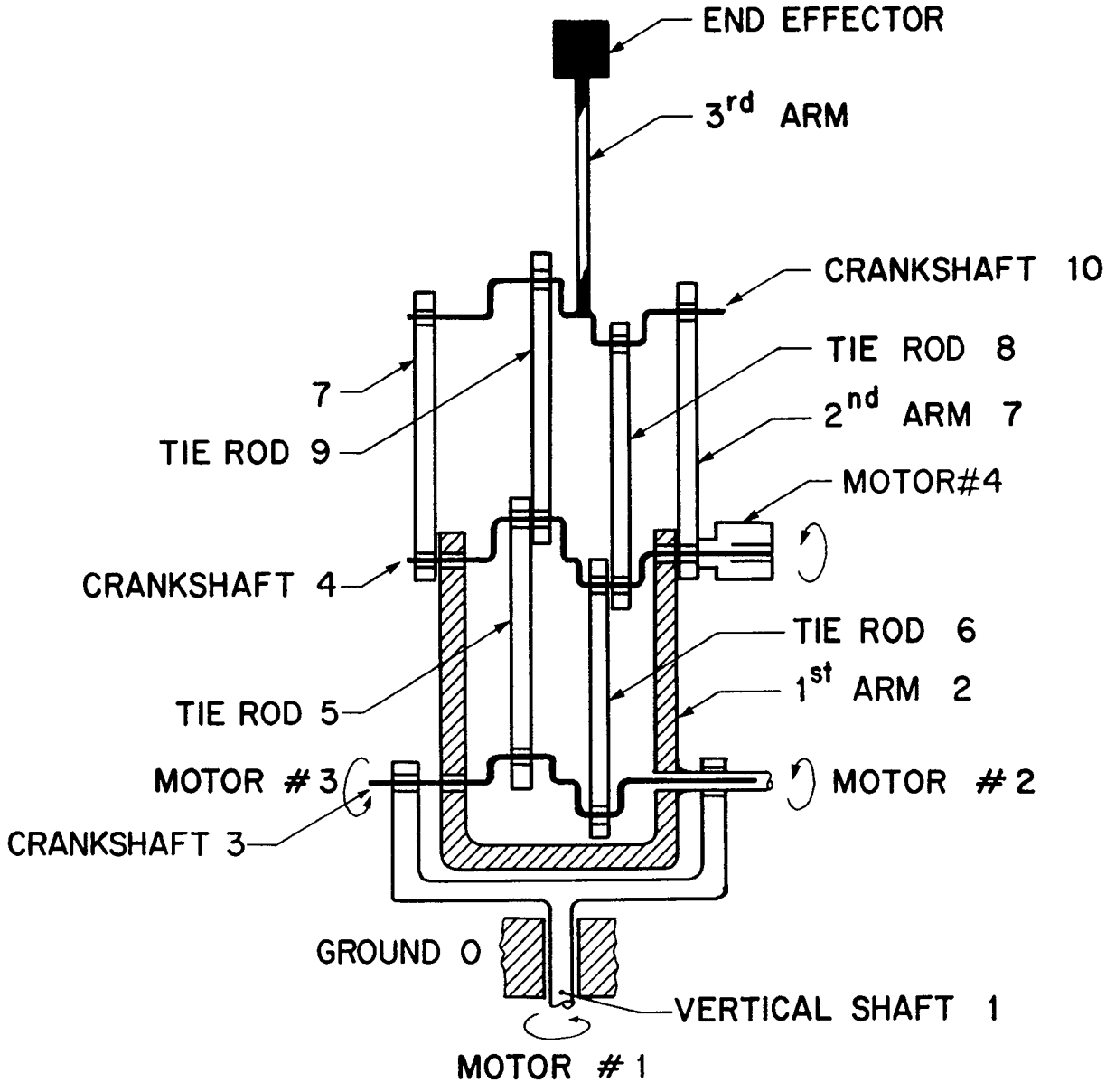
END EFFECTOR
3rd ARM
CRANKSHAFT 10
TIE ROD 8
7
2nd ARM 7
TIE ROD 9
MOTOR#4
CRANKSHAFT 4
TIE ROD 6
1st ARM 2
TIE ROD 5
MOTOR #3
MOTOR #2
CRANKSHAFT 3
GROUND 0
VERTICAL SHAFT 1
MOTOR #1

Fig. 4

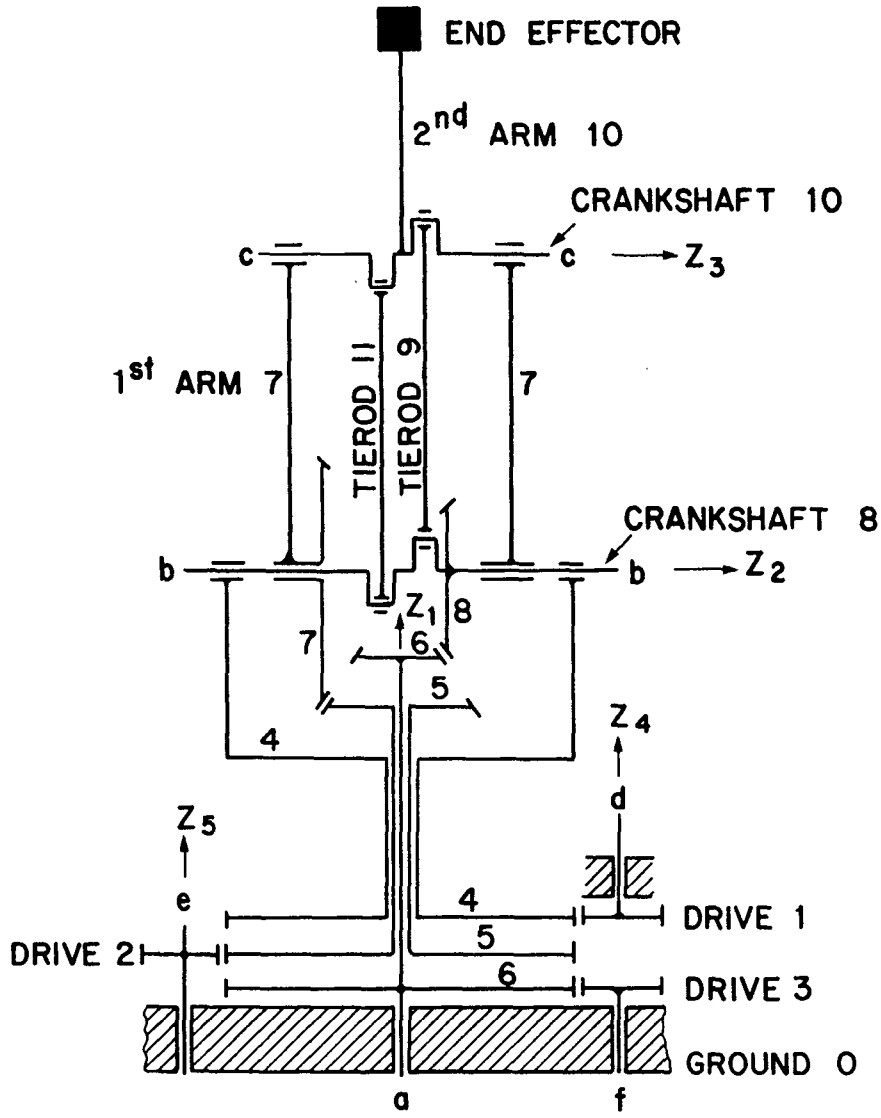
END EFFECTOR
2nd ARM 10
CRANKSHAFT 10
c
c
Z3
1st ARM 7
TIEROD 11
TIEROD 9
7
CRANKSHAFT 8
b
b
Z2
Z1
8
7
6
5
4
Z4
d
Z5
e
4
DRIVE 1
DRIVE 2
5
6
DRIVE 3
GROUND 0
a
f

Fig. 5a

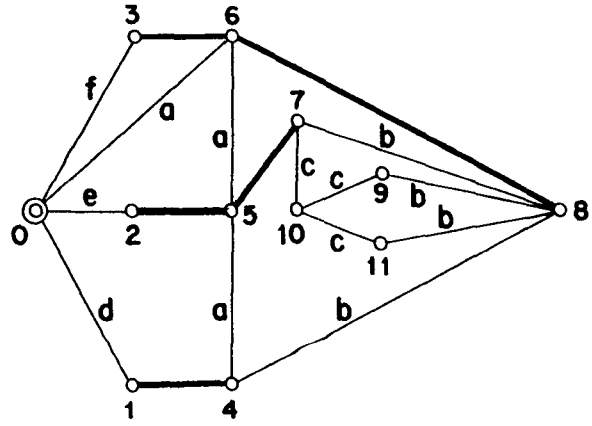
3
6
f
a
a
7
b
c
c
9
b
b
e
0
2
5
10
c
11
8
d
a
b
1
4

Fig. 5b

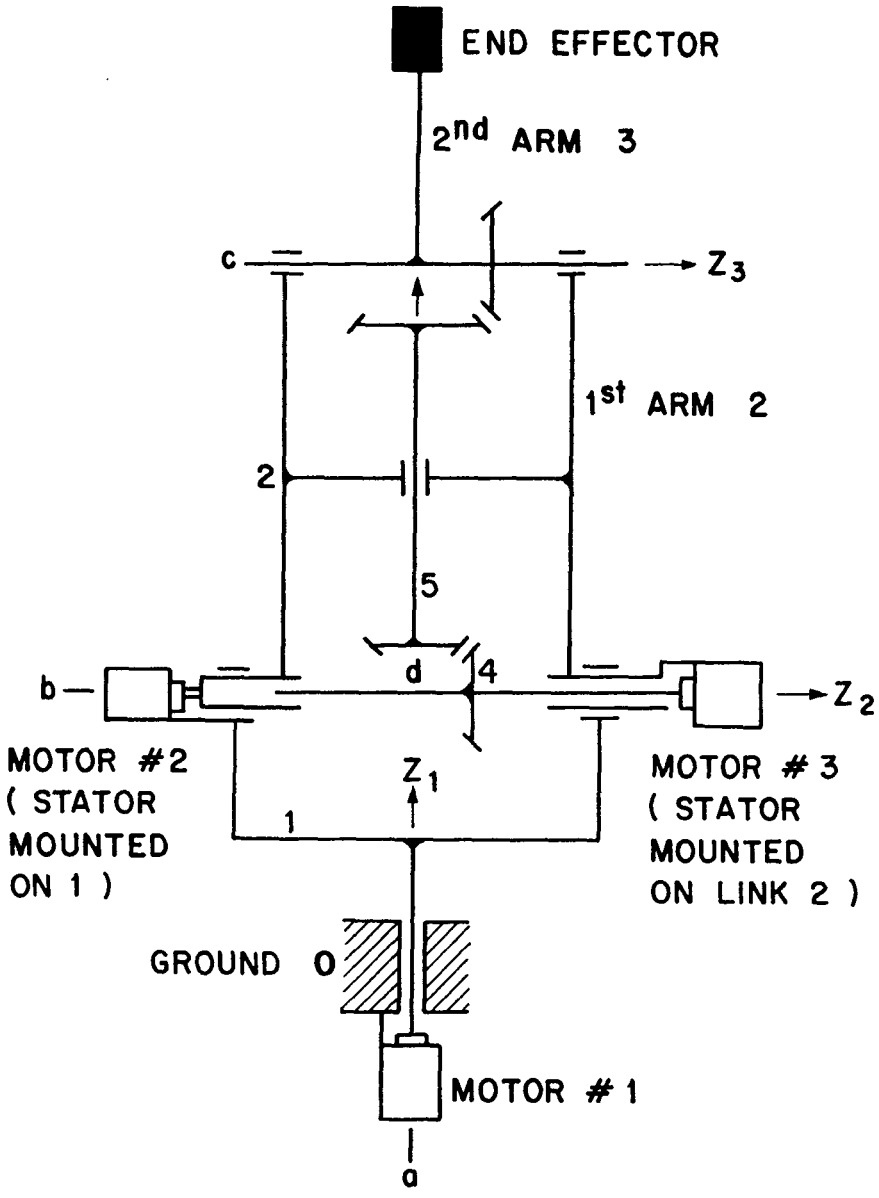
END EFFECTOR
2nd ARM 3
c
Z3
1st ARM 2
2
5
d
4
b
Z2
MOTOR #2
(STATOR
MOUNTED
ON 1)
Z1
1
MOTOR # 3
(STATOR
MOUNTED
ON LINK 2)
GROUND 0
MOTOR # 1
a

Fig. 6a

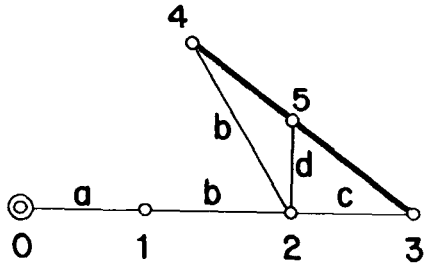
4
5
b
d
a
b
c
0
1
2
3

Fig. 6b

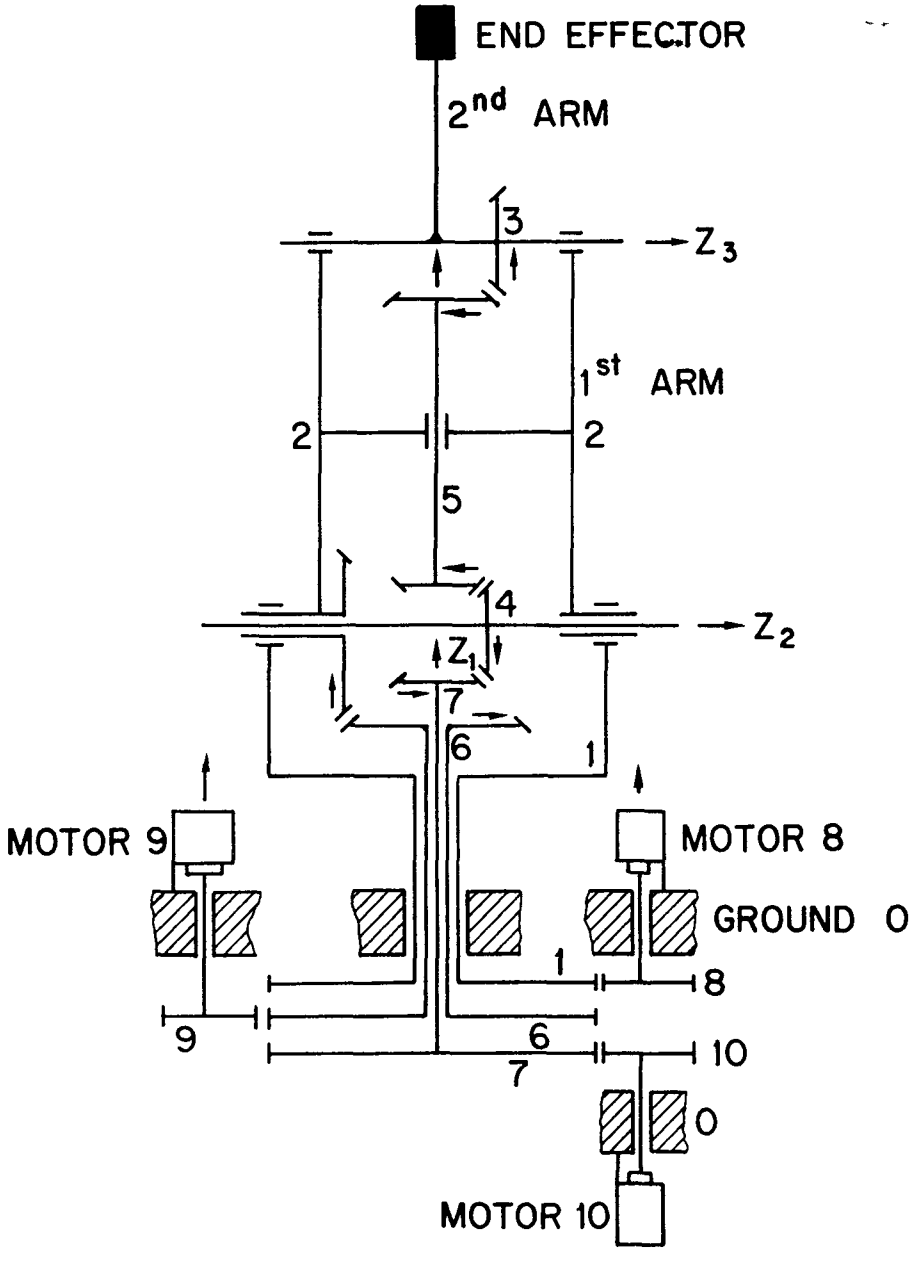
END EFFECTOR
2nd ARM
3
Z3
1st ARM
2
2
5
4
Z2
Z1
7
6
1
MOTOR 9
MOTOR 8
GROUND 0
1
8
9
6
10
7
0
MOTOR 10

Fig. 7